

Relaxational dynamics study of the classical Heisenberg spin XY model in spherical coordinate representation

Beom Jun Kim and Petter Minnhagen

Department of Theoretical Physics, Umeå University, 901 87 Umeå, Sweden

Suhk Kun Oh and Jean S. Chung

Department of Physics, Chungbuk National University, Cheongju 361-763, Korea

The two- and three-dimensional classical Heisenberg spin XY (CHSXY) model, with the spherical coordinates of spins taken as dynamic variables, are numerically investigated. We allow the polar (θ) and azimuthal (ϕ) angles to have uniform values in $[0, \pi)$ and $[-\pi, \pi)$, respectively, and the static universality class is shown to be identical to the classical XY model with two-component spins, as well as the CHSXY model with different choice of dynamic variables, conventionally used in the literature. The relaxational dynamic simulation reveals that the dynamic critical exponent z is found to have value $z \approx 2.0$ for both two and three dimensions, in contrast to $z \approx d/2$ (d = spatial dimension) found previously with spin dynamics simulation of the conventional CHSXY model. Comparisons with the usual two-component classical XY model are also made.

PACS numbers: 75.40.Gb, 75.40.Mg, 64.60.Ht

I. INTRODUCTION

The static critical behaviors of the XY model in two (2D) and three dimensions (3D) have been studied for more than twenty years and there exist well-established consensus on the nature of the phase transitions and the values of the critical exponents.^{1,2} For example, static universal properties have been well established where the static exponents do not depend on details of models. On the other hand, the dynamic universality class has still not been completely sorted out.^{2,3}

The usual XY model, where the spins are two dimensional, has been found to have dynamic critical exponents z which seem to depend both on which dynamic model is used and on which quantity is measured.⁴ In 2D most of the existing works have obtained the result that $z \approx 2.0$ at the Kosterlitz-Thouless transition¹ temperature T_{KT} and that z increases as the temperature T is lowered below T_{KT} .^{2,3,5-9} However, the result that $z \approx 2.0$ in the whole low-temperature phase has also been found.^{10,11} In 3D, on the other hand, there is a growing consensus that the dynamic critical exponent z associated with voltage (or phase slip) fluctuations is $z \approx 1.5$ (Refs. 7,12-14) although a rigorous analytic justification is still lacking. Furthermore this appears to be the case even for relaxational dynamics in spite of the fact that $z \approx 2.0$ has been concluded from standard dynamic renormalization group method (for example, in Ref. 15) in accordance with model A in the Hohenberg-Halperin classification.¹⁶

The variant of the XY model, which we study here, is given by a Hamiltonian of the same form as the usual XY model but where the spins are three dimensional [we call this the classical Heisenberg spin XY model (CHSXY) to avoid confusion with the usual XY model]. This model has previously been studied subject to the so-called “spin dynamics”.¹⁷⁻¹⁹ Although the CHSXY model belongs to the same static universality class as the XY model both in 2D (Ref. 20) and 3D (Ref. 21), studies of spin dynamics for the CHSXY model have given $z \approx 1.0$ in 2D,¹⁷ which differs significantly from

$z \approx 2.0$ in the XY model. In 3D, while Ref. 18 has found $z \approx 1.5$, the possibility of a breakdown of the dynamic scaling has been suggested, i.e., that z is not unique but has different values $z_x = 1.38(5)$ and $z_z = 1.62(5)$ for the decay of correlations in the in-plane and the out-of-plane directions, respectively.¹⁹

We here propose a variant of the CHSXY model where the spherical coordinates of the spins are taken as the dynamic variables with a uniform measure in phase space, and investigate the dynamic critical behaviors of the model in two and three dimensions subject to relaxational dynamics instead of spin dynamics. Relaxational dynamics belongs to the model A with the expected value $z \approx 2$ in the Hohenberg-Halperin classification.¹⁶ However, this value does not always seem to be guaranteed. For example, the purely relaxational form of dynamics applied to the XY model in 3D under the fluctuating twist boundary condition has been found to give $z \approx 1.5$ (Ref. 12). Even the Monte Carlo (MC) dynamics simulations, which are generally believed to correspond to relaxational dynamics, for the 3D XY model with both phase⁴ and vortex¹³ representation has also led to $z \approx 1.5$.

The paper is organized as follows: In Sec. II, the Hamiltonian of the CHSXY model in the spherical coordinate representation and the corresponding equations of motion for the relaxational dynamics are introduced. Although our main interests are in dynamic critical behaviors we also perform Monte Carlo simulations in Sec. III to confirm the equivalence with the conventional CHSXY model and then compare with static and dynamic results from the relaxational dynamics in Sec. IV, which constitutes the main results of the current work. Finally we devote Sec. V for summary and discussions.

II. MODEL

We begin with the Hamiltonian of the conventional CHSXY model in the d -dimensional hypercubic geometry

with size $N = L^d$ (L is the linear size):

$$H[\{s^x, s^y\}] = -J \sum_{\langle ij \rangle} (s_i^x s_j^x + s_i^y s_j^y), \quad (1)$$

where J is the coupling strength, the summation is over all nearest-neighbor pairs, and the three dimensional local spin $\mathbf{s}_i = (s_i^x, s_i^y, s_i^z)$ at site i has unit length ($|\mathbf{s}_i|^2 = 1$), or equivalently the partition function should include the measure $\delta[(s_i^x)^2 + (s_i^y)^2 + (s_i^z)^2 - 1]$. The CHSXY model with the Hamiltonian (1) can be viewed as either an extension from the original XY model where spins are two dimensional, or as a special case of the Heisenberg XXZ model with couplings only in the x - y plane.

The more convenient representation of the conventional CHSXY Hamiltonian is written as

$$H[\{s^z, \phi\}] = -J \sum_{\langle ij \rangle} \sqrt{[1 - (s_i^z)^2][1 - (s_j^z)^2]} \cos(\phi_i - \phi_j), \quad (2)$$

where $(s_i^x)^2 + (s_i^y)^2 = 1 - (s_i^z)^2$ has been used, and ϕ_i is the angle between the x - y plane component of the spin \mathbf{s}_i , i.e., $\mathbf{s}_i - s_i^z \hat{\mathbf{z}}$, and the positive x axis. In this representation (2), ϕ and s^z have uniform measure since

$$\begin{aligned} & \int ds^x \int ds^y \int ds^z \delta[(s^x)^2 + (s^y)^2 + (s^z)^2 - 1] \\ &= \int ds^z \int r dr \int d\phi \delta[r^2 + (s^z)^2 - 1] \\ &\propto \int_{-1}^1 ds_z \int_{-\pi}^{\pi} d\phi, \end{aligned} \quad (3)$$

where $r^2 \equiv (s^x)^2 + (s^y)^2$, $\phi \equiv \arctan(s^y/s^x)$, and the identity $\delta(r^2 - a^2) = \delta(r - a)/2r$ has been used.

We in present work introduce the polar angle variable θ in the spherical coordinate system as follows:

$$\begin{aligned} s_i^x &= \sin \theta_i \cos \phi_i, \\ s_i^y &= \sin \theta_i \sin \phi_i, \\ s_i^z &= \cos \theta_i, \end{aligned} \quad (4)$$

which then leads to the representation

$$H[\{\theta, \phi\}] = -J \sum_{\langle ij \rangle} \sin \theta_i \sin \theta_j \cos(\phi_i - \phi_j). \quad (5)$$

We then simplify the conventional CHSXY model and use the *uniform* measure not only for ϕ but also for θ variables. One advantage of this is that no additional constraint is required since $|\mathbf{s}_i| = 1$ is satisfied automatically in the representation (5). One should note that the conventional CHSXY model [represented by the Hamiltonian (2) with the uniform measure in s^z and ϕ] and its variant model studied in this work [the Hamiltonian (5) with the uniform measure in θ and ϕ]²² do not have the same partition function and free energy and accordingly some nonuniversal properties like the critical

temperature can be different. However, one expects that universal critical properties should be the same as will be clearly confirmed in Sec. III below.

The relaxational dynamic equations are simply given by⁶

$$\begin{aligned} \dot{\theta}_i &= -\Gamma \frac{\partial H[\{\theta, \phi\}]}{\partial \theta_i} + \eta_i^\theta, \\ \dot{\phi}_i &= -\Gamma \frac{\partial H[\{\theta, \phi\}]}{\partial \phi_i} + \eta_i^\phi, \end{aligned} \quad (6)$$

where Γ is a constant which determines the time scale of relaxation, and the stochastic thermal noise terms satisfy $\langle \eta_i^\theta(t) \rangle = \langle \eta_i^\phi(t) \rangle = \langle \eta_i^\theta(t) \eta_j^\theta(t') \rangle = 0$ and $\langle \eta_i^\theta(t) \eta_j^\theta(t') \rangle = \langle \eta_i^\phi(t) \eta_j^\phi(t') \rangle = 2T \delta_{ij} \delta(t - t')$ with the ensemble average $\langle \dots \rangle$. (From now on, we measure the temperature T and the time t in units of J/k_B and $1/\Gamma J$, respectively.) From the Fokker-Planck (F-P) formalism, it is straightforward to show that the stationary solution of F-P equation, corresponding to the above Langevin-type equations of motion (6), is simply the equilibrium Boltzmann distribution with the Hamiltonian given in Eq. (5). In other words, the relaxational dynamics used in this work automatically produces equilibrium fluctuations in time, which are compatible with the Boltzmann distribution of the same Hamiltonian. In this respect, the initial configuration of the relaxational dynamics can be chosen arbitrarily; the equilibrium fluctuations are generated by the dynamics itself as the system evolves in time. This is in contrast to the widely used spin dynamics, where the initial configurations must be generated according to the equilibrium distribution. Otherwise the spin dynamics will not reflect the properties of the equilibrium. Consequently, the relaxational dynamics described here is consistent with the usual physical situation of a system in contact with a thermal reservoir. From this perspective we believe that the relaxational dynamics can phenomenologically catch relevant features for a real spin system in situation when the thermal effects are strong.

III. MONTE CARLO SIMULATION

For completeness we start by calculating the static properties from MC simulations within the spherical coordinate $(\{\theta, \phi\})$ representation with both variables uniformly distributed, which we have not found in the literature. We use the standard Metropolis algorithm applied to the Hamiltonian (5), and the variations of θ_i and ϕ_i at each MC try are tuned to give acceptance ratio about one half near the critical temperature. Later we will compare the MC results with those from the relaxational dynamics in Sec. IV.

A. Three-Dimensional Lattice

In 3D, the transition is detected by the order parameter defined as²¹

$$\langle m \rangle \equiv \left\langle \frac{1}{N} |\mathbf{S}| \right\rangle = \left\langle \frac{1}{N} \sqrt{S_x^2 + S_y^2 + S_z^2} \right\rangle, \quad (7)$$

where the total spin vector \mathbf{S} is given by

$$\mathbf{S} = \sum_{i=1}^N \mathbf{s}_i. \quad (8)$$

The most convenient way to locate the critical temperature T_c is to calculate the Binder's fourth-order cumulant

$$U_L(T) = 1 - \frac{\langle m^4 \rangle}{3\langle m^2 \rangle^2}, \quad (9)$$

which has a unique crossing point as a function of T if plotted for various system sizes. Figure 1 shows the determination of T_c from the Binder's cumulant for the system size $L = 4, 6, 8, 10, 12$, and 16 in 3D and $T_c = 1.256(1)$ is obtained. As expected, this value of T_c is found to be different than $T_c = 1.552(1)$ obtained from the other choice of variables in Hamiltonian (2) with uniform measures for s^z and ϕ .^{18,19,21} However, one expects that such a change cannot alter the universality class of the system. As an example we compute the static critical exponent ν , which is defined by $\xi \sim (T - T_c)^{-\nu}$ and can be calculated from

$$U_L(T) \approx U^* + U_1 L^{1/\nu} \left(1 - \frac{T}{T_c} \right), \quad (10)$$

where U^* is also a universal value and found to be $U^* = 0.586(1)$ from Fig. 1. Equation. (10) is written in a more convenient form:

$$\Delta U_L = U_L(T_1) - U_L(T_2) \propto L^{1/\nu}, \quad (11)$$

where T_1 and $T_2 (> T_1)$ are picked near T_c . In the inset of Fig. 1, ΔU_L is plotted as a function of system size L in the log scale with $T_1 = 1.25$ and $T_2 = 1.26$, and $\nu = 0.67(3)$ is obtained. The values of ν and U^* obtained here

$$\nu = 0.67(3), \quad (12)$$

$$U^* = 0.586(1), \quad (13)$$

are within error bars in agreements with the known values for the the conventional CHSXY model with the uniform measure for s^z and ϕ : $\nu = 0.670(7)$, $U^* \approx 0.586$ in Ref. 21 (the latter was estimated from Fig. 1 in Ref. 21), and $\nu = 0.669(6)$, $U^* = 0.5859(8)$ in Ref. 19. This just illustrates that the change of variables and measures in phase space introduced in Sec. II does not change the static universality class although the critical temperature T_c is found to be different.

B. Two-Dimensional Lattice

In many 2D systems with continuous symmetry, the spontaneous magnetization vanishes at any nonzero temperature and the phase transition of the XY model and its related models is of the Kosterlitz-Thouless type.¹ Figure 2 shows the specific heat C_v , computed from $C_v = (\langle H^2 \rangle - \langle H \rangle^2)/T^2 N$, for the 2D CHSXY model in the spherical coordinate representation versus T for various system sizes $L = 4, 6, 8, 10, 12, 16, 24$,

and 32. The C_v peak for the KT transition is characterized by a finite peak height in the limit of infinite size, which is consistent with Fig. 2. We then compute the in-plane susceptibility χ defined as²⁰ (see Fig. 3)

$$\chi \equiv (\chi_x + \chi_y)/2, \quad (14)$$

where the susceptibility in the α direction ($\alpha = x, y$) is written as

$$\chi_\alpha = \frac{1}{N} \left\langle \left(\sum_i s_\alpha^i \right)^2 \right\rangle. \quad (15)$$

The in-plane susceptibility χ can be used to determine the critical temperature T_c : We use the relation $\chi \sim L^{2-\eta}$ and the condition that the exponent η has value $1/4$ at T_c , and obtain $T_c = 0.621(3)$ (see the inset of Fig. 3). It is again to be noted that $T_c = 0.621(3)$ obtained here for the 2D CHSXY model in the spherical coordinate representation is different from $T_c = 0.699(3)$ obtained in Ref. 20 for the conventional CHSXY model.

IV. RELAXATIONAL DYNAMICS SIMULATION

In the relaxational dynamics simulations in both 3D and 2D, we use the second-order Runge-Kutta-Helfand-Greenside (RKHG) algorithm²³ and the equations of motion in Eq. (6) are integrated numerically with the discrete time step $\Delta t = 0.05$. The relaxational dynamics with the representation $\{\theta, \phi\}$ used here (see Sec. II) is more convenient than the representation $\{s^z, \phi\}$ since no constraint on θ_i and ϕ_i is required while the constraint $|s_i^z| \leq 1$ should be explicitly fulfilled in the latter representation. After neglecting initial transient behaviors, ensemble averages of static physical quantities can be computed from the time averages of those quantities, due to the ergodicity of the system. In contrast to the spin dynamics method,¹⁷⁻¹⁹ where initial configuration for dynamic calculation should be generated from the MC simulation, one can in relaxational dynamics take any initial configuration to start with; as time proceeds, the dynamics intrinsically generates equilibrium fluctuations.

A. Three-Dimensional Lattice

We first present the static results in 3D. Figure 4 shows the determination of T_c from the Binder's cumulant [see Eqs. (9) and (10)]: the crossing point gives $T_c = 1.245(2)$ and $U^* = 0.585(3)$. In dynamic simulations the inevitable finite time step Δt causes an effective shift of the temperature (see Ref. 6 for discussions). Of course in the limit of $\Delta t \rightarrow 0$ this temperature shift vanishes⁶ and the critical temperatures determined from dynamic simulation and MC simulation become identical. The effective temperature shift in the RKHG algorithm used here is much smaller than the simple Euler algorithm, and the deviation in T_c in the current 3D case is less

than 1%. Within numerical accuracy we find that U^* computed from relaxational dynamics (see Fig. 4) agrees with that from MC in Sec. III A, and thus also with values in Refs. 21 and 19. We display the determination of the critical exponent ν for the relaxational dynamics in the inset of Fig. 4, where $\nu = 0.66(6)$ is obtained (compare with Fig. 1 for MC in 3D). The values of ν and U^* found from the relaxational dynamics of the 3D CHSXY model in the spherical coordinate representation again confirm that the static universality class of the model is identical to the usual 3D XY universality class.

We next investigate the dynamic critical behaviors. One convenient way of characterizing the dynamic universality class is to compute the total spin time correlation function $G(t)$ defined as¹⁸

$$G(t) \equiv \frac{\langle S_x(t)S_x(0) + S_y(t)S_y(0) \rangle}{\langle S_x^2(0) + S_y^2(0) \rangle}, \quad (16)$$

where the total spin vector $\mathbf{S} = (S_x, S_y, S_z)$ is given in Eq. (8) and the $\langle \dots \rangle$ is substituted by the time average in the relaxational dynamics study. Since $G(t=0) = 1$ at any T and L , the finite-size scaling of $G(t)$ is written in a very simple form:

$$G(t, L, T) = g(tL^{-z}, (T - T_c)L^{1/\nu}), \quad (17)$$

where the first scaling variable is the ratio between the time t and the characteristic time scale $\tau \sim L^z$ with the dynamic critical exponent z , and the second scaling variable comes from the ratio between the system size L and the coherence length $\xi \sim (T - T_c)^{-\nu}$ with the static critical exponent ν .

At $T = T_c$, the above scaling form reduces to a simpler form with a single scaling variable

$$G(t, L, T_c) = g(tL^{-z}, 0), \quad (18)$$

and all G 's at different system sizes should collapse to a single curve once the correct value of z is chosen. In Fig. 5, G at $T = 1.25$ is shown (a) as a function of the time t and (b) as a function of the scaling variable tL^{-z} with $z = 2.0$. All curves at different sizes $L = 4, 6, 8, 10$, and 12 are shown to collapse relatively well to a single curve with the dynamic critical exponent $z = 2.0$, although the quality of the collapse is not perfect: This is because $T = 1.25$ and $z = 2.0$ chosen in Fig. 5 can be slightly different from the true T_c and z (see below for a more precise determination).

The other implication of the above finite-size scaling form with two scaling variables in Eq. (17) is that if the first scaling variable is fixed to a certain constant value $a \equiv tL^{-z} = \text{constant}$ it again reduces to a simple form:

$$G(t, L, T) = g(a, (T - T_c)L^{1/\nu}). \quad (19)$$

It then suggests that when G 's with fixed a at different system sizes are plotted as functions of T , all curves should cross at a single point at $T = T_c$ if the correct value of z is chosen; this provides an independent method to determine T_c (and z at the same time). Figure 6 displays this intersection plot with $z = 2.05$ and $a = 0.53$ (this value of a , with which the intersection occurs at $G \approx 0.5$, is taken only as an example; in

a broad range of a the similar intersection plot is achieved). We try different values of z and a , and it is concluded that $z = 2.05(5)$ and $T_c = 1.245(3)$, the latter of which is in an agreement with the previously determined value from the Binder's cumulant in Fig. 4.

In summary of this section, the relaxational dynamics study applied for the 3D CHSXY model in the spherical coordinate representation has revealed that this model belongs to the 3D XY static universality class characterized by $\nu \approx 0.67$ and $U^* \approx 0.586$, while the dynamic critical exponent has value $z \approx 2.0$. We note that this value $z \approx 2$ is in accord with the model A in the Hohenberg-Halperin classification¹⁶ as well as with $z \approx 2.015$ found from the dynamic renormalization group calculation in Ref. 15. On the other hand, many studies on the 3D XY model with the resistively shunted junction dynamics,^{7,12,14} the relaxational dynamics^{7,12} under the fluctuating twist boundary condition,⁶ and the MC dynamics for both phase⁴ and vortex¹³ representations have observed $z \approx 1.5$. Also, the spin dynamics for the conventional 3D CHSXY model also has yielded z 's which are significantly different from value 2: $z \approx 1.5$ in Ref. 18, and $z_x \approx 1.38(5)$ and $z_z = 1.62(5)$ in Ref. 19

B. Two-Dimensional Lattice

The static results obtained from the time averages during the numerical integrations of the relaxational dynamic equations of motion (6) in 2D are first presented. The specific heat $C_v = (\langle H^2 \rangle - \langle H \rangle^2)/T^2 N$ with $N = L^2$, and the in-plane susceptibility χ in Eqs. (14) and (15) are exhibited as functions of the temperature T in Figs. 8 and 9, respectively. As expected, the static calculations from the relaxational dynamics simulations result in basically the same results as from the MC simulations in Figs. 2 and 3 in Sec. III B. From χ in Fig. 9, we locate T_c in the inset of Fig. 9 in the same way as in Fig. 3 in Sec. III B, through the use of $\chi \sim L^{2-\eta}$ with $\eta = 1/4$ at T_c . In 2D, we find $T_c = 0.621(3)$, which is identical to T_c found from MC simulation in Fig. 3 within numerical errors.

We next turn to the investigation of the dynamic universality class of the 2D CHSXY model in the spherical coordinate representation under the relaxational dynamics. In general, the 2D systems with the KT transition are quasicritical in the whole low-temperature phase. This means that when $T \leq T_c$ we cannot use the finite-size scaling form in Eq. (17) since the coherence length ξ is infinite. In 2D, we then write the scaling form for $T \leq T_c$ as follows:

$$G(t, T, L) = g(tL^{-z(T)}), \quad (20)$$

where the dynamic critical exponent $z(T)$ is allowed to vary with temperature. (More precisely, the scaling function g should also depend on T). Figure 10(a) displays the total spin time correlation function G in Eq. (16) at $T = 0.62$ as a function of the time t for various system sizes $L = 4, 6, 8, 10$, and 12 . If we put $z = 2.0$ in Eq. (20) all curves in Fig. 10(a) collapse to a single curve as shown in Fig. 10(b). Consequently,

we conclude that the 2D CHSXY model in the spherical coordinate representation under relaxational dynamics has the dynamic critical exponent $z \approx 2.0$ at T_c . We show in Fig. 10(c) and (d) the similar scaling plot at $T = 0.50$ which is significantly lower than T_c . Interestingly, we again find $z \approx 2.0$ at $T = 0.50$, which suggests that this model has $z \approx 2.0$ in the whole low-temperature phase.

In many existing analytical and simulational studies of the 2D XY model in its original form, $z(T)$ has been found to have value 2 at T_c , and to increase as T is decreased.^{2,3,5-9} Since $z(T)$ can also be related with the nonlinear IV exponent a by $a(T) = z(T) + 1$, which is usually measured in experiments, there are also experimental papers with the same conclusion.²⁴ In contrast, there exist studies with other conclusions: For example, in Ref. 10 the decay from nonequilibrium to equilibrium (this technique is often called “short time relaxation method”) in the MC dynamics has been found to result in $z(T) \approx 2$ at any T below T_c , and the same has been concluded in Ref. 7 from the similar short time relaxation method but applied for the relaxational dynamics of the XY model. Also in Ref. 11, the scaling of the total spin correlation function has been investigated in the same way as in the present paper, and $z \approx 2$ in the whole low-temperature phase has been concluded for the relaxational dynamics of the 2D XY model.

The spin dynamics study of the conventional 2D CHSXY model in Ref. 17 has obtained $z \approx 1.0$ which is close to $z = d/2$ ($d = 2$ in 2D) for the model E value in Hohenberg-Halperin classification.¹⁶ While the models in Ref. 17 and in the present work belong to the same static universality class, they do not need to belong to the same dynamic universality class: In spin dynamics, the z component S_z of the total spin is a constant of motion since the Hamiltonian H commutes with the spin operator in the z direction. On the other hand, the relaxational dynamics is not based on this commutation relation, and S_z is not a conserved quantity.

Although 2D and 3D CHSXY model have the same z , it should be kept in mind that their critical behaviors are completely different: In 2D, the whole low-temperature phase is quasicritical and one can associate $z(T)$ at each temperature to make G at different sizes collapse to a single curve as displayed in Fig. 10. In 3D, on the other hand, the system is critical only at T_c and the curve collapse with the single scaling variable tL^{-z} as shown in Fig. 5 is not found at any other temperatures.

V. SUMMARY

We in this paper have investigated the static and the dynamic universality class of the two- and three-dimensional CHSXY model where three-dimensional classical spins interact with each other through the Hamiltonian with only in-plane components coupled.

The spherical polar (θ) and azimuthal (ϕ) angles of the spin direction, both with uniform measures in phase space, are taken as dynamic variables, which leads to the simple re-

laxational dynamic equations of motion since the constraint $|\mathbf{s}_i| = 1$ is fulfilled automatically. It is to be noted that the relaxational dynamics method makes it possible to study both the dynamic and the static properties on the same footing, in contrast to the spin dynamics method. In other words, in the spin dynamics method initial configurations for dynamic calculation should be generated from the MC simulation, while one can in relaxational dynamics take any initial configuration to start with; the relaxational dynamics intrinsically generates equilibrium fluctuations as the system evolves in time.

From the static calculations based on the relaxational dynamics method it was explicitly verified that both the 2D and 3D CHSXY models in the spherical coordinate representations belong to the expected 2D and 3D XY static universality classes, respectively. The dynamic critical exponent z has been found to be different from values obtained from various other existing studies of the XY model including relaxational dynamics. The value $z \approx 2.0$ found here for both 2D and 3D implies that the relaxational dynamics of the CHSXY model is governed by the model A description in Hohenberg-Halperin classification.¹⁶

ACKNOWLEDGMENTS

BJK thanks for the hospitality during his visit at Chungbuk National University, where this work was begun. This work was supported by the Swedish Natural Research Council through Contract No. F 5102-659/2001 (BJK and PM), and SKO and JSC were supported by the Korea Research Foundation through grant KRF-99-005-D00034.

-
- ¹ J. M. Kosterlitz and D. J. Thouless, J. Phys. C **5**, L124 (1972); **6**, 1181 (1973); V. L. Berezinskii, Zh. Eksp. Teor. Fiz. **61**, 1144 (1972) [Sov. Phys. JETP **34**, 610 (1972)].
 - ² P. Minnhagen, Rev. Mod. Phys. **59**, 1001 (1987).
 - ³ V. Ambegaokar, B. I. Halperin, D. R. Nelson, and E. Siggia, Phys. Rev. Lett. **40**, 783 (1978); Phys. Rev. B **21**, 1806 (1980).
 - ⁴ P. Minnhagen, B. J. Kim, and H. Weber (unpublished).
 - ⁵ B. J. Kim, Phys. Rev. B **63**, 024503 (2001).
 - ⁶ B. J. Kim, P. Minnhagen, and P. Olsson, Phys. Rev. B **59**, 11506 (1999).
 - ⁷ L. M. Jensen, B. J. Kim, and P. Minnhagen, Phys. Rev. B **61**, 15412 (2000).
 - ⁸ K. Holmlund and P. Minnhagen, Phys. Rev. B **54**, 523 (1996).
 - ⁹ H. Weber, M. Wallin, and H. Jensen, Phys. Rev. B **53**, 8566 (1996).
 - ¹⁰ A. J. Bray, A. J. Briant, and D. K. Jervis, Phys. Rev. Lett. **84**, 1503 (2000); H. J. Luo and B. Zheng, Mod. Phys. Lett. B **11**, 615 (1997).
 - ¹¹ S. K. Kim and J. S. Chung (unpublished).
 - ¹² L. M. Jensen, B. J. Kim, and P. Minnhagen, Europhys. Lett. **49**,

- 644 (2000); B. J. Kim, L. M. Jensen, and P. Minnhagen, *Physica B* **284**, 413 (2000).
- ¹³ H. Weber and H. J. Jensen, *Phys. Rev. Lett.* **78**, 2620 (1997); J. Lidmar, M. Wallin, C. Wengel, S. M. Girvin, and A. P. Young, *Phys. Rev. B* **58**, 2827 (1998).
- ¹⁴ K. H. Lee and D. Stroud, *Phys. Rev. B* **46**, 5699 (1992).
- ¹⁵ R. A. Wickham and A. T. Dorsey, *Phys. Rev. B* **61**, 6945 (2000).
- ¹⁶ P. C. Hohenberg and B. I. Halperin, *Rev. Mod. Phys.* **49**, 435 (1977).
- ¹⁷ H. G. Evertz and D. P. Landau, *Phys. Rev. B* **54**, 12302 (1996); S. K. Oh, C. N. Yoon, J. S. Chung, and S.-C. Yu, *J. Appl. Phys.* **81**, 3986 (1997).
- ¹⁸ S. K. Oh, C. N. Yoon, and J. S. Chung, *Phys. Rev. B* **56**, 13677 (1997); *J. Korean Phys. Soc.* **34**, 117 (1999); (unpublished).
- ¹⁹ M. Krech and D. P. Landau, *Phys. Rev. B* **60**, 3375 (1999).
- ²⁰ A. Cuccoli, V. Tognetti, and R. Vaia, *Phys. Rev. B* **52**, 10221 (1995).
- ²¹ K. Nho and E. Manousakis, *Phys. Rev. B* **59**, 11575 (1999).
- ²² Throughout this paper, the CHSXY model represented by the Hamiltonian (2) with s^z and ϕ subject to uniform measure in phase space is referred as “the conventional CHSXY model”, while we call the model (5) with the uniform measures for θ and ϕ “the CHSXY model in the spherical coordinate representation”, for convenience.
- ²³ G. G. Batrouni, G. R. Katz, A. S. Kronfeld, G. P. Lepage, B. Svetitsky, and K. G. Wilson, *Phys. Rev. D* **32**, 2736 (1985).
- ²⁴ See, e.g., Refs. 2 and 9 for comparisons with experiments.

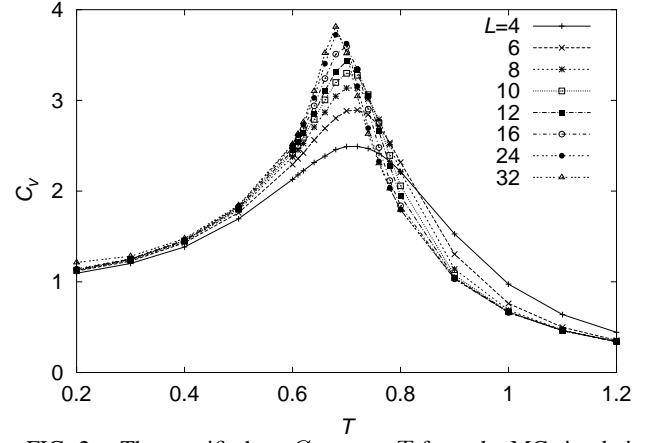


FIG. 2. The specific heat C_v versus T from the MC simulation of the 2D CHSXY model in the spherical coordinate representation for various system sizes $L = 4, 6, 8, 10, 12, 16, 24$, and 32 ; the specific heat peak appears to saturate as L is increased.

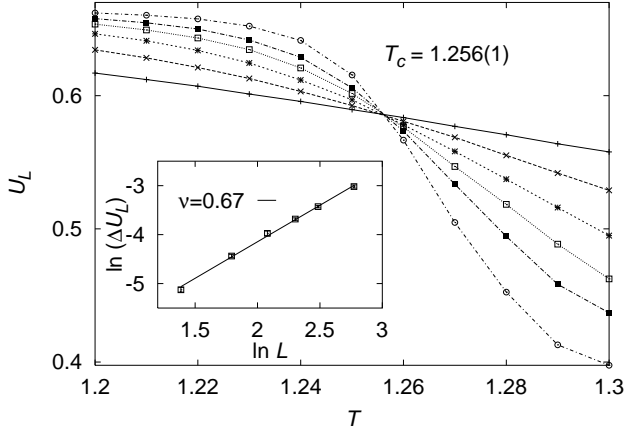


FIG. 1. Fourth order Binder's cumulant U_L for the 3D CHSXY model in the spherical coordinate representation from MC simulations as a function of the temperature T for various system sizes $L = 4, 6, 8, 10, 12$, and 16 (from top to bottom on the right hand side of the crossing point). The crossing point gives the estimation of the critical temperature $T_c = 1.256(1)$. Inset: Determination of the critical exponent ν through the finite-size scaling of U_L . $\Delta U_L \equiv U_L(T = 1.25) - U_L(T = 1.26)$ (see text for details). From the least-square fit $\nu = 0.67(3)$ is obtained.

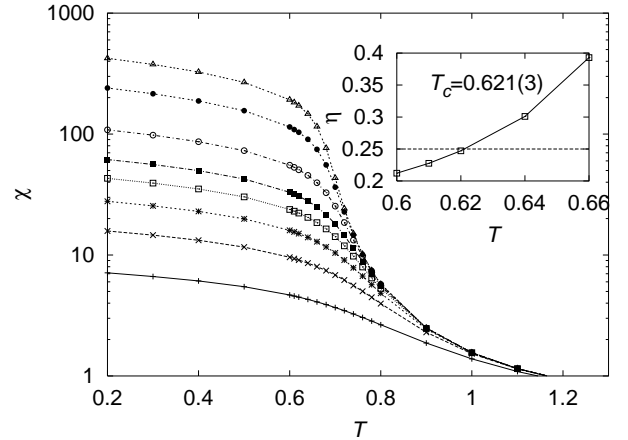


FIG. 3. In-plane susceptibility χ from MC simulation in 2D versus temperature T at system sizes $L = 4, 6, 8, 10, 12, 16, 24$, and 32 (from bottom to top). Inset: The exponent η , obtained from $\chi(T, L) \sim L^{2-\eta(T)}$ is shown as a function of T . From the condition that $\eta(T_c) = 1/4$, $T_c = 0.621(3)$ is found.

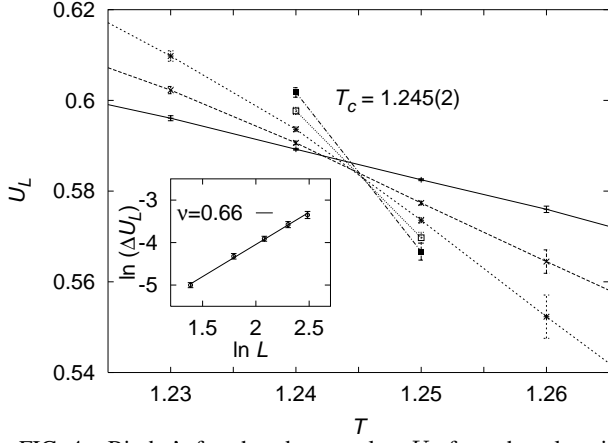


FIG. 4. Binder's fourth order cumulant U_L from the relaxational dynamics simulation in 3D as a function of T for $L = 4, 6, 8, 10$, and 12 (from top to bottom on the right hand side of the crossing point). The crossing point gives the estimation $T_c = 1.245(2)$. Inset: Determination of ν from the least-square fit; $\nu = 0.66(6)$ is obtained (to be compared with Fig. 1 for MC).

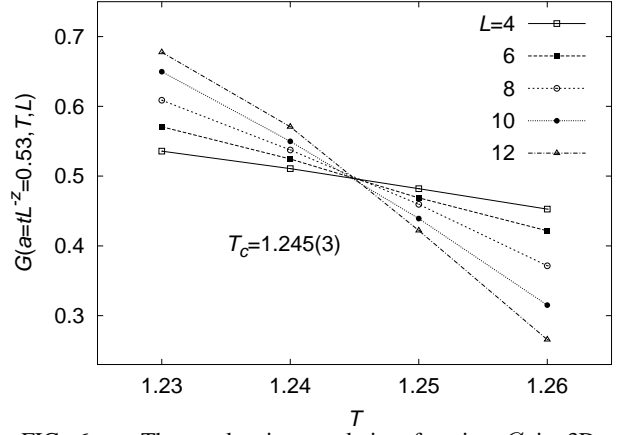


FIG. 6. The total spin correlation function G in 3D with $a \equiv tL^{-z} = 0.53$ ($z = 2.05$) is shown as a function of temperature T for various system sizes $L = 4, 6, 8, 10$, and 12 . All curves cross at $T \approx 1.245$, which is in a very good agreement with $T_c = 1.245(2)$ found in static calculation with relaxational dynamics (see Fig. 4). The value of $a = 0.53$ is chosen only for convenience ($a = 0.53$ makes the intersection occurs at $G \approx 0.5$); in a broad range of a , the quality of this intersection plot is very good if $z = 2.05$ is chosen. The other values of z and a are tried and $z = 2.05(5)$ and $T_c = 1.245(3)$ are concluded.

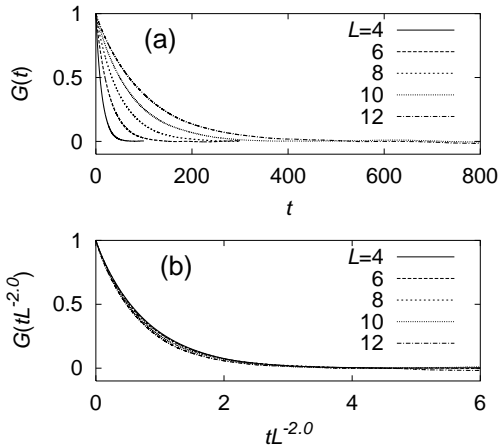


FIG. 5. Total spin correlation function G from relaxational dynamics in 3D at $T = 1.25$ is shown for $L = 4, 6, 8, 10$, and 12 , as a function of (a) the time t and (b) the scaling variable tL^{-z} with $z = 2.0$. The curve collapse in (b) implies that $T_c \approx 1.25$ and $z \approx 2.0$. See Figs. 6 and 7 for more precise determination of T_c and z .

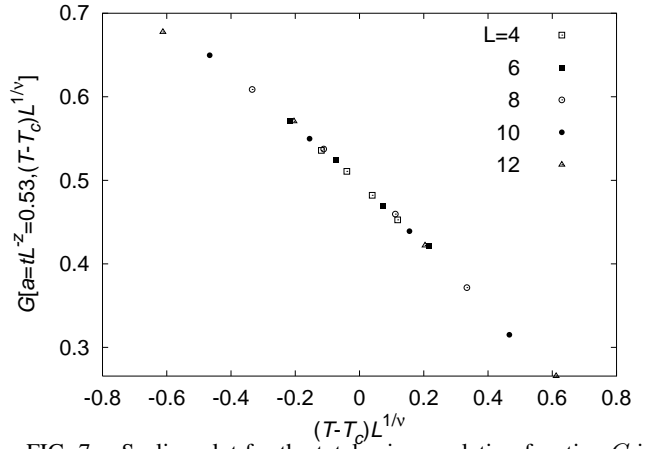


FIG. 7. Scaling plot for the total spin correlation function G in 3D with $a \equiv tL^{-z} = 0.53$ and $z = 2.05$. All data points in Fig. 6 collapse to a smooth curve with $T_c = 1.245$ and $\nu = 0.67$. The quality of the curve collapse at different a values are similar to this one in a broad range of a .

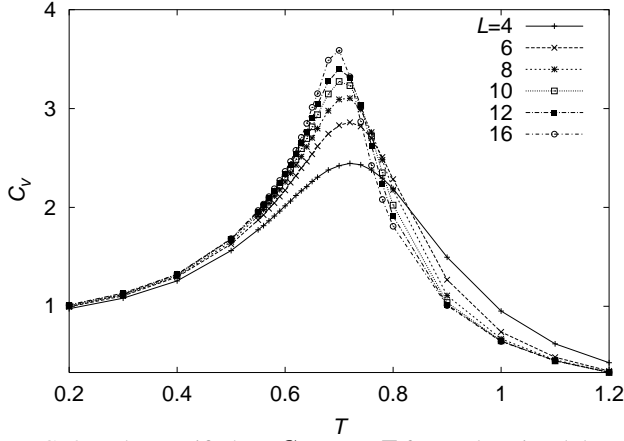


FIG. 8. The specific heat C_v versus T from relaxational dynamics simulation in 2D for various system sizes $L = 4, 6, 8, 10, 12$, and 16 (from bottom to top). (Compare with Fig. 2 which has been obtained from independent MC simulations.)

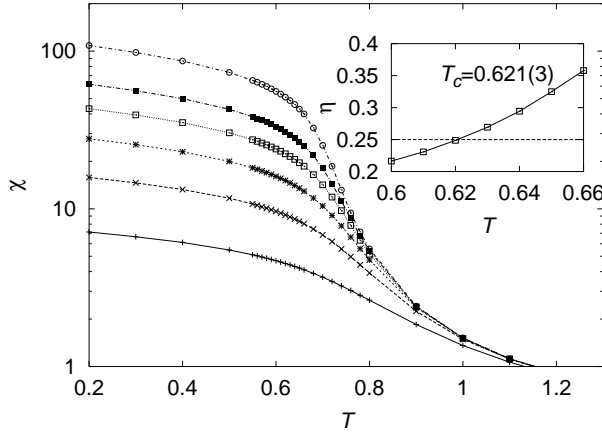


FIG. 9. In-plane susceptibility χ from relaxational dynamic simulation in 2D versus temperature T for various system sizes $L = 4, 6, 8, 10, 12$, and 16 . As expected, the relaxational dynamics simulations give quantitatively similar curves (compare with Fig. 3). Inset: The exponent η as a function of T is displayed and $T_c = 0.621(3)$ is found. (Compare with Fig. 3 for MC.)

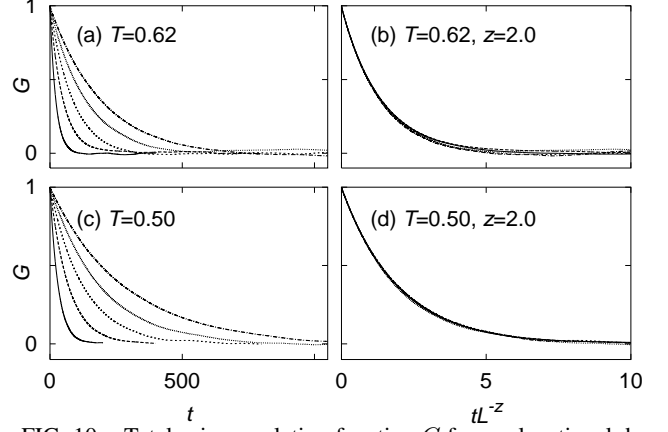


FIG. 10. Total spin correlation function G from relaxational dynamic simulation in 2D at (a) $T = 0.62 \approx T_c$ and (c) $T = 0.50$ as a function of the time t for $L = 4, 6, 8, 10$, and 12 (from left to right); (b) and (d) display the corresponding scaling plots with the scaling variable tL^{-z} and $z \approx 2.0$ is found at both $T = 0.62$ and 0.50 , implying that $z(T) \approx 2.0$ in the whole low-temperature phase.